ACS Sustainable Chemistry & Engineering

pubs.acs.org/journal/ascecg

Letter

New Material Perspective for Waste Seashells by Covalent Functionalization

Giulia Magnabosco,*[,‡] Demetra Giuri,[‡] Anna Paola Di Bisceglie, Francesco Scarpino, Simona Fermani, Claudia Tomasini,* and Giuseppe Falini*

Cite This: *ACS Sustainable Chem. Eng.* 2021, 9, 6203–6208

Read Online

ACCESS | Metrics & More | Article Recommendations | Supporting Information

ABSTRACT: Seashells are a calcium-carbonate-based material that can be converted into valuable advanced functional materials. Seashells are also a waste material from aquaculture. They are produced in millions of tonnes per year and represent an environmental issue. They uniquely contain an intraskeletal organic matrix rich in carboxylate groups that so far has not been exploited or has been even removed, when they were used as calcium carbonate substitutes. The intraskeletal organic matrix allows for a so far never reported covalent functionalization. Such a process strengthens the surface functionalization with respect to adsorption and, most importantly, opens up the possibility for the functionalization of the biogenic calcium carbonate with a wide variety of molecules by means of organic chemistry reactions. As a proof of concept, powdered waste oyster shells were covalently functionalized with a fluorescent probe. The impact of this research can be terrific in the valorization of $CaCO_3$ from biogenic wastes providing advanced functional products tailored for individual applications. Moreover, its consequences on the environment and society will epitomize a perfect example of a circular economy.

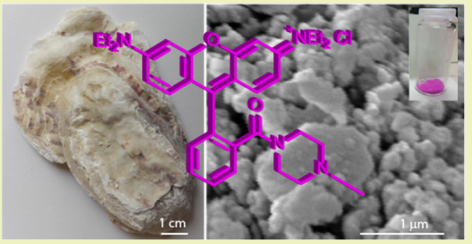

KEYWORDS: *Seashells, Waste, Oyster, Calcium carbonate, Biomaterials, Pollution, Chemical functionalization*

INTRODUCTION

Calcium carbonate ($CaCO_3$) has extensive applications as a filler in the pharmaceutical, adhesive, construction, polymer, and paper industries and many others. Currently, $CaCO_3$ originates primarily from geological sources, which can contain heavy metals or other impurities difficult to remove.[1] Moreover, extraction of $CaCO_3$ from quarries has a negative environmental and visual impact and, when the need for site regeneration is taken into account, leads to higher extraction costs.[2] Although $CaCO_3$ can be synthesized in laboratories and industrial plants (precipitated $CaCO_3$, PCC),[3] allowing a higher degree of control over the composition, shape, and size of the particles, the high cost of synthesis (×100 higher) makes this prohibitively expensive, and quarries have remained the main source of $CaCO_3$.[4] An additional challenge is that when $CaCO_3$ is used as a filler in composites, it generally reduces the mechanical performance of the host material. One way of overcoming this is by creating physiochemical interactions between $CaCO_3$ and the host material. To strengthen the interaction, various molecules can be physiochemically adsorbed onto $CaCO_3$.[5] However, such adsorption is limited to a specific class of molecules able to interact with the $CaCO_3$ particle surfaces, and desorption can occur. De Reese et al. showed that the adsorption of comb charged polymers occurs by entropy gain, whereas linear charged polymers adsorb because of strong electrostatic interactions with the $CaCO_3$ surface.[6] PCCs were coated with stearic acid in an aqueous medium with the coating amount ranging from 3 to 13.5 wt %. It was found that the calcium stearate formed on the coated surface was only partially chemisorbed and that a complete chemisorbed monolayer was not obtained.[7] An inorganic coating of $CaCO_3$ was performed using silica.[8] In this research, eight silane coupling agents showed very different effects on the mechanical properties of polypropylene/$CaCO_3$ composites. Amino-functional silane coupling agents adhere well to the $CaCO_3$ surface and react also with the polymer. This concept was used to improve mechanical properties of $CaCO_3$ based resin compounds in which waste materials (seashells, limestone aggregates, concrete, and limestone dust) were used as a source of $CaCO_3$.[9]

Covalent, chemical functionalization of inorganic/organic composite biogenic $CaCO_3$ particles can overcome the limitations associated with adsorption and provide new $CaCO_3$ based materials. In this work, we introduce the use of biogenic $CaCO_3$ derived from mollusk shells that (*i*) are a more environmentally sustainable source of $CaCO_3$ than quarries and industrial plants and (*ii*) inherently contain macromolecules within their structure that can be uniquely

Received: February 26, 2021
Revised: April 8, 2021
Published: April 23, 2021

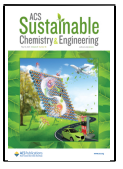

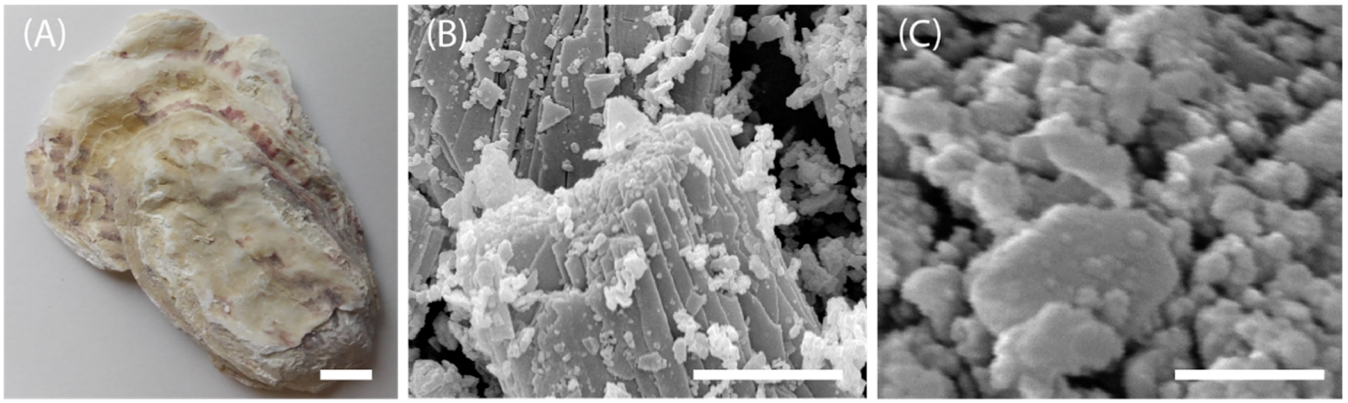

Figure 1. (A) Camera image of a valve of oyster *C. gigas* from waste materials. (B) SEM images of fractured shell of oyster *C. gigas* (B) and of powdered oyster shell (C). Scale bars are (A) 1 cm, (B) 10 μm, and (C) 1 μm.

tailored with functional groups of choice by covalent functionalization.

As source of biogenic $CaCO_3$, we used the shells of the oyster *Crassostrea gigas* (Figure 1A), which is one of the most important aquacultural species, with an overall production above 0.5 Mton/year.[10] Before commercialization, 15 wt % of shells is discarded by the production chain as unwanted waste, the vast majority of them being either landfilled or dumped in the sea, causing a significant environmental impact.[11] Oyster shells are made of $CaCO_3$ in the form of low magnesium calcite with an isomorphic substitution of magnesium to calcium of about 5 mol %.[12] Both valves of the adult oyster shell are predominantly composed of foliated calcite, which is bound on the outermost surface by prismatic calcite and is interrupted by lenses of chalky calcite.[13,14] Figure 1 shows a shell of an oyster (Figure 1A), a fragment of fractured shell (Figure 1B), and a shell powder obtained after ball milling (Figure 1C). The foliated texture is eliminated by the ball milling process, leading to spherical particles.

Powdered oyster shells have been used in several applications, mainly after thermal decarbonation to calcium oxide, thus removing the intraskeletal organic matrix.[15,16] An efficient and recyclable waste oyster shell powder-supported CuBr catalyst was used in the synthesis of triazole derivatives. It showed higher catalytic activity compared with a $CaCO_3$–CuBr due to the chelating effect of the organic matrix.[17] Zhou et al. coated oyster shell particles with a polydopamine network taking advantage of the positive effects of texture (high surface area and submicron porosity) on the polymerization of polydopamine.[18] However, so far, no attention has been dedicated to the covalent functionalization of oyster shell particles, as well of other biogenic calcium carbonates, exploiting the organic matrix.[16]

To achieve the goal of a covalent functionalization, we developed a scalable methodology that converts mollusk shell powders (e.g., waste oyster shells) into a new generation of advanced functional biomineral based materials. Rhodamine B (Rho-B) was used as probe molecule since it has a high emission yield and can be easily detected by spectroscopic techniques.[19]

Since the organic matrix of $CaCO_3$ biominerals contains glycoproteins with a high content of amino acids bearing carboxylate groups (i.e., aspartate and glutamate),[20,21] the synthetic strategy was focused on the exploitation of this functional group, which is expected to be exposed on the surface of the biogenic $CaCO_3$ particles due to its hydrophilicity.

RESULTS AND DISCUSSION

To fully take advantage of the overall compositional and functional features of biogenic $CaCO_3$, or any biomineral in general, it is fundamental to preserve the organic–inorganic structural organization across the nano- and microscales of oyster shells, especially during the handling and grinding stages. First, the shells were treated with sodium hypochlorite to remove organic residues on the surface of the valve and ensure that only the intracrystalline organic matrix is exposed after grinding and is available for functionalization. Then, the shells were ground using a crusher mill and a planetary ball mill in sequence, producing particles with an average diameter (D_{50}) of 3.7 μm (D_{98} = 27 μm) and a surface area of 4.29 m^2/g (Figure SI1). We verified that this process did not alter the content of intraskeletal material, an organic matrix and water, in the oyster shell particles. Thermogravimetric analysis showed that the content of the intraskeletal material within the mortar and pestle ground oyster shell powder (1.3 ± 0.1 wt %) did not change after the ball milling process (1.1 ± 0.2 wt %; Figure SI2). These data agree with previous data reported for oyster shells.[21] We also verified that there was no change in the mineral phase during the milling process. In fact, the X-ray diffraction pattern and the FTIR spectrum revealed that only magnesium calcite was present after the grinding (Figure SI3). Particular attention was paid to the evaluation of the protein content exposed on the surface of the biogenic particles of $CaCO_3$. Such quantification was performed using the BCA method on pristine ground biogenic $CaCO_3$ particles and on the same particles after prolonged oxidative degradation of the surface proteins using sodium hypochlorite.[22] This is a colorimetric method based on the complexation by bicinchoninic acid of Cu^+ obtained from the protein reduction of Cu^{2+}. The relative quantification was performed using a calibration curve obtained with BSA. The obtained data were expressed as a mass percentage of surface protein over the mass of the biogenic calcium carbonate. The relative quantification gave a result of 0.28 ± 0.02 wt % for the untreated particles and 0.03 ± 0.02 wt % for the bleached particles (Table 1). These latter data indicate the absence of surface protein after sodium hypochlorite oxidative treatment. This material was used as a control instead of synthetic/geogenic $CaCO_3$ since (i) it had exactly the same elemental composition, (ii) the same particle

https://doi.org/10.1021/acssuschemeng.1c01306
ACS Sustainable Chem. Eng. 2021, 9, 6203–6208

Table 1. Mass Percentage of Surface Proteins on Covalently Functionalized Pristine Oyster Shell Powder and the One Bleached with Sodium Hypochlorite[a]

	oyster shell powder	bleached oyster shell powder
surface proteins (wt %)	0.28 ± 0.02	0.03 ± 0.02
linked Rho-B (wt %)[b]	0.06 ± 0.02	0.02 ± 0.01

[a]The percentage refers to the mass of the oyster shell powder. [b]The percentage of linked Rho-B was obtained by a spectrophotometric analysis upon dissolution of the calcium carbonate in a 50 mM acetate buffer at pH 4.5 (details in the SI).

size distribution is not obtainable with synthetic/geogenic $CaCO_3$, and (iii) it has been reported that the synthetic/geogenic $CaCO_3$ has higher chemical stability and lower porosity than the biogenic one.[23,24] It was also decided not to use oyster powder as a control after the heat treatment that removes the organic matrix, as this process generates additional porosity.[25] Subsequently, the coupling reaction of Rho-B piperazine (Figure 2, detailed procedure in SI) with oyster shell particles was set up following an optimized experimental procedure.[26,27] Our idea was to form a peptide bond between the free amine group of the Rho-B piperazine (using piperazine as a linker) and the exposed carboxyl groups of the protein, mostly due to the presence of glutamic and aspartic acid moieties.

The powder from oyster shells was dried for about 1 h in the oven at 60 °C to remove moisture. Then, a portion of $CaCO_3$ powder (260 mg corresponding to 0.7 mg of organic material) was suspended in dry acetonitrile (18 mL). A large excess of the coupling reagent HBTU (hexafluorophosphate benzotriazole tetramethyl uronium; 1.1 equiv, 0.286 mmol) was added to the mixture; then the dispersion was kept under stirring in an inert N_2 atmosphere for 10 min at room temperature. Successively, a solution of Rho-B piperazine (1 equiv, 0.260 mmol; synthesis in SI) and DIEA (*N*,*N*-diisopropylethylamine; 3 equiv, 0.780 mmol) dissolved in dry acetonitrile was added to the oyster shell powder treated with the coupling reagent, and the reaction was stirred under an inert atmosphere for 2 h. The obtained covalent functionalized oyster shell powder was then filtered and washed with ethyl acetate (three washes of 10 mL). Finally, the obtained material was dried in an oven at 60 °C (Figure 3). The same procedure was applied to oyster shells from which surface proteins were removed by sodium hypochlorite treatment (260 mg; Figure 3).

The amount of Rho-B present on the pristine oyster powder shell (covalent functionalization and adsorption) and on the bleached oyster powder shell (only adsorption) was determined by UV−visible spectroscopy after dissolving the $CaCO_3$ in an acetate buffer 50 mM at pH 4.5. A calibration curve was used and the absorption was measured at 558 nm (see SI). The results are reported in Table 1. The higher content of Rho-B on the pristine sample is visible by the naked eye (Figure 3) and was quantified to be 0.06 ± 0.02 wt %, while in the bleached sample, it was 0.02 ± 0.01 wt %. This last datum shows an increase of 0.04 wt % of Rho-B, which we ascribed to the covalent functionalization on the surface of the particles.

The oyster shell powder structure was characterized after the coupling reaction. The FTIR and X-ray diffraction (Figure SI4) analyses were performed on both powders of oyster shell, pristine and bleached. The results showed that the functionalization procedure did not change the phase composition. The images of samples observed by scanning electron microscopy showed that the powders did not change their morphology or aggregation during the functionalization process (Figure 3), being similar to those from the pristine oyster powder shells (Figure 1). This was expected since the functionalization process was performed in solvents in which $CaCO_3$ is insoluble, and therefore its dissolution and reprecipitation processes and concomitant effects were absent.

Confocal microscope observations were performed on the two types of powders subjected to the functionalization process and on the pristine oyster powder. The images show that the particles treated with Rho-B are strongly fluorescent (Figure 4B,C), as expected. Furthermore, even the untreated powder shows a slight fluorescence (Figure 4A), which can be associated with the intraskeletal organic material.[28] However, using the same experimental setup, the fluorescence of the uncontaminated sample is negligible compared to that of those treated with Rho-B. Furthermore, the images show that the fluorescence on the functionalized particles is not homogeneous, and some regions appear more fluorescent than others. This latter observation agrees with a heterogeneous distribution of the intraskeletal organic matrix.[29,30] Indeed, we can suppose that during the grinding process the shell breaks with a glassy fracture, as well as along cleavage planes.[31] This gives rise to regions exposing a higher concentration of organic matrix molecules than others. Furthermore, we cannot exclude the formation of multilayers of Rho-B in some regions of the particles (e.g., kinks) as already reported for the adsorption of Rho-B on clays[32] and palm shell activated carbon,[33] among many examples.

An estimate of the density of Rho-B molecules located on the surface of powdered oyster shells in their pristine state or after the treatment to remove surface proteins was performed. About one molecule per 5 nm^2 and one molecule per 15 nm^2 were calculated on the pristine and treated samples, respectively. This rough estimation was simply performed considering the moles of Rho-B per gram of powder, and thus the number of molecules, and the surface per gram of particles. Since the molecular size of Rho-B is approximately 1.44 nm × 1.09 nm × 0.64 nm,[34] a molecule of Rho-B covers a surface of about 1.5 nm^2, i.e., about six molecules per 10 nm^2. This rough evaluation indicates that Rho-B molecules cover no more than

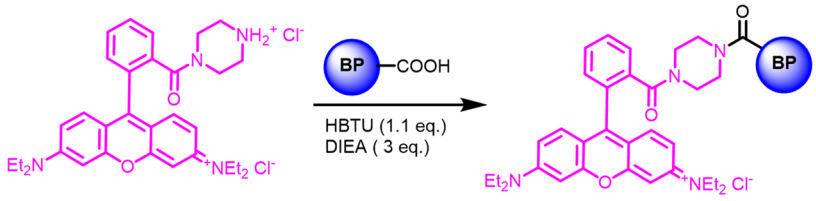

Figure 2. Reaction of functionalization of the oyster shell particle (BP) with Rho-B piperazine molecule.

https://doi.org/10.1021/acssuschemeng.1c01306
ACS Sustainable Chem. Eng. 2021, 9, 6203−6208

Figure 3. (A) SEM image of bleached oyster powder (shown in the vial) after chemical functionalization with Rho-B. (B) SEM image of the pristine oyster powder (shown in the vial) after chemical functionalization with Rho-B. Scale bar is 1 μm.

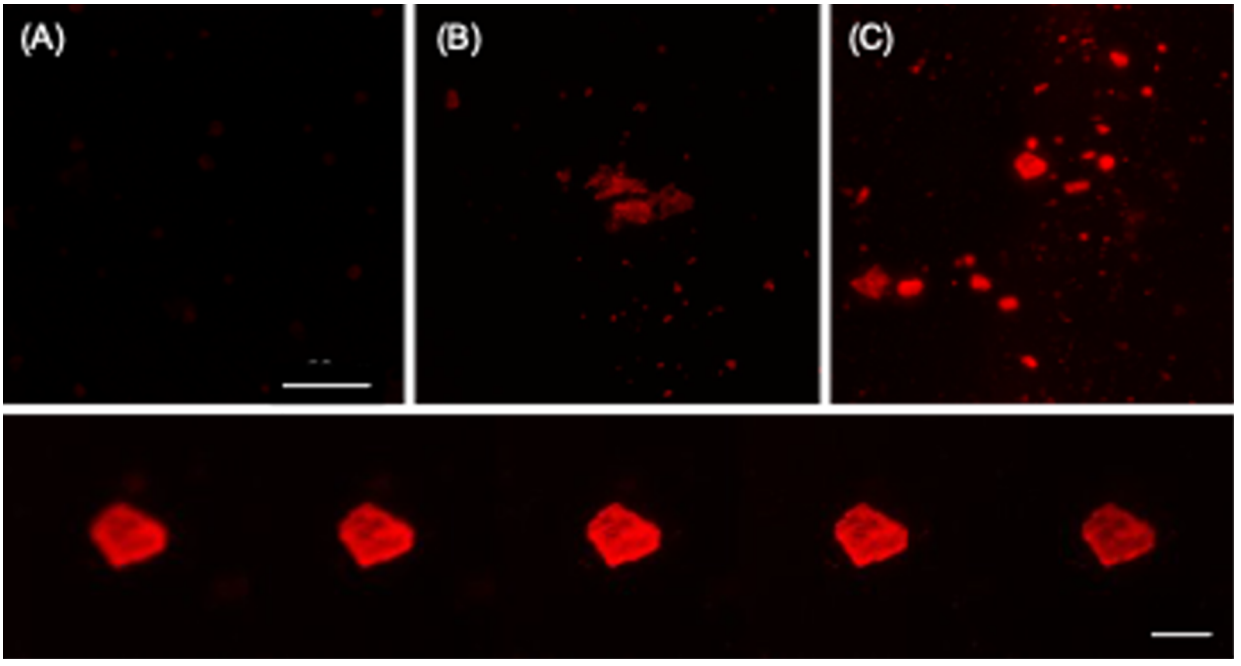

Figure 4. (Top) Confocal microscopy images of the pristine oyster powder shell (A), of the functionalized oyster powder shell after bleaching with sodium hypochlorite (B), and of the functionalized pristine oyster powder shell. The three images are at the same magnification and were acquired using the same experimental setup. Scale bar is 50 μm. (Bottom) Confocal imaging (slices) of a Rho-B covalently functionalized oyster shell particle. Scale bar is 10 μm.

about 1/60 of the powder's surface. However, considering that the confocal microscopy observations suggest the presence of multilayers,[32,33] or at least an inhomogeneous surface distribution of Rho-B, this value could be overestimated. The density of carboxylate groups per unit surface area is difficult to quantify, because of their low concentration and the structural and compositional complexity of the oyster shell powder. It has been reported that XPS spectra of oyster shell powder revealed only a weak N 1s signal and a C 1s spectrum, but unfortunately these signals cannot be used for a quantitative analysis.[18] To overcome these limitations, we used the BCA method.[22]

This method allowed us to confirm the absence of surface proteins, and therefore carboxylate groups, on the surface of the bleached samples but did not allow the quantifiation of the yield of the coupling reaction and evaluation of the organization of the Rho-B molecules on the oyster shell powder.

To gain further information on the presence of the organic matrix molecules in the oyster powder after chemical functionalization with Rho-B, we analyzed two samples of oyster powder by ^{1}H NMR spectroscopy. Twenty milligrams of pristine oyster powder was suspended in D_2O (0.7 mL), then DCl (40 μL) was added to the mixture. The same procedure was performed on the same amount of bleached oyster powder. The ^{1}H NMR analysis of the two samples is reported in Figure 5 and testifies to the presence of aromatic hydrogens (between 7 and 8 ppm) on both samples and may be ascribed to the Rho-B moiety.

These signals have been highlighted with a purple frame. In the sample obtained from the pristine oyster powder (Figure 5 top), we recorded several peaks ranging between 1 and 5 ppm, typical of aliphatic hydrogens that are perfectly in agreement with the presence of peptide chains of the organic matrix. These signals have been highlighted with a blue frame and are not present in the spectrum recorded with the bleached oyster

https://doi.org/10.1021/acssuschemeng.1c01306
ACS Sustainable Chem. Eng. 2021, 9, 6203−6208

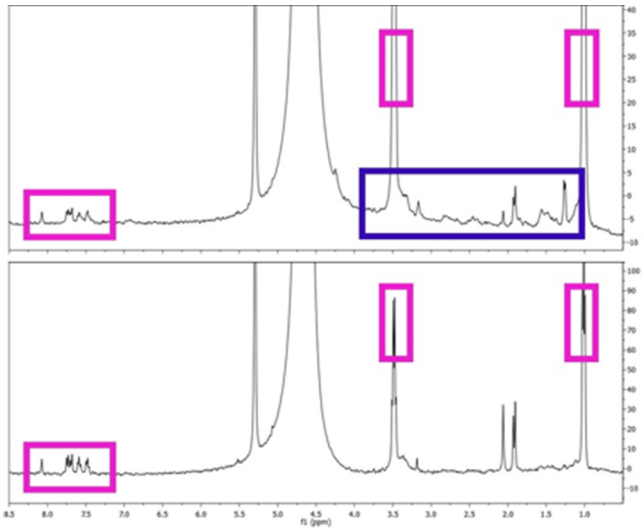

Figure 5. ^{1}H NMR spectra of oyster powders in D_2O recorded at 400 MHz. DCl was added to dissolve $CaCO_3$: (top) spectrum of dissolved pristine oyster powder; (bottom) spectrum of the bleached oyster powder. The purple frames highlight the signals ascribed to Rho-B, while the blue frame highlights the signal ascribed to the organic matrix. Some sharp peaks recorded around 2.0 and 5.5 ppm can be ascribed to the reaction solvents. The large peak at 4.6 ppm is due to water.

powder. Some sharp peaks recorded around 2.0 and 5.5 ppm can be ascribed to the reaction solvents. The large peak at 4.6 ppm is due to water.

CONCLUSIONS

In summary, we have shown for the first time that the organic matrix can be exploited to functionalize biominerals, biogenic $CaCO_3$ particles in our case, by forming a covalent bond on specific functional groups of the organic matrix. Such functionalization is not possible with geogenic or synthetic $CaCO_3$, which do not contain entrapped organic molecules. Our research demonstrated the potential for such an approach, leading us to expect that a similar synthetic strategy can be used with different (macro)molecules to create limitless types of tailor-made functionalization for specific applications, preserving the astonishing properties of mollusk shells, by leaving unaltered the textural organization of the biogenic $CaCO_3$ on the submicron-scale.[35] The impact of this research can be terrific in the valorization of $CaCO_3$ from biogenic wastes, providing a new family of materials to be used both in the current $CaCO_3$ application sectors and in the new ones. Finally, the valorization of waste seashells from aquaculture represents a perfect example of a circular economy and will provide innovative materials tailored for customer applications.

ASSOCIATED CONTENT

Supporting Information

The Supporting Information is available free of charge at https://pubs.acs.org/doi/10.1021/acssuschemeng.1c01306.

Materials and methods used for the preparation of the covalently functionalized powdered oyster shells; synthesis and characterization of the rhodamine B−piperazine molecule; particle size distribution of the oyster shell powder; content of intraskeletal material determined by TGA analysis; determination of the mineral phase of the oyster shell powders by X-ray diffraction and FTIR spectroscopy (PDF)

AUTHOR INFORMATION

Corresponding Authors

Giulia Magnabosco − *Dipartimento di Chimica "Giacomo Ciamician", Alma Mater Studiorum Università di Bologna, 40126 Bologna, Italy;* orcid.org/0000-0003-1552-773X; Email: giuseppe.falini@unibo.it

Claudia Tomasini − *Dipartimento di Chimica "Giacomo Ciamician", Alma Mater Studiorum Università di Bologna, 40126 Bologna, Italy;* orcid.org/0000-0002-6310-2704; Email: claudia.tomasini@unibo.it

Giuseppe Falini − *Dipartimento di Chimica "Giacomo Ciamician", Alma Mater Studiorum Università di Bologna, 40126 Bologna, Italy;* orcid.org/0000-0002-2367-3721; Email: giulia.magnabosco@fau.de

Authors

Demetra Giuri − *Dipartimento di Chimica "Giacomo Ciamician", Alma Mater Studiorum Università di Bologna, 40126 Bologna, Italy*

Anna Paola Di Bisceglie − *Dipartimento di Chimica "Giacomo Ciamician", Alma Mater Studiorum Università di Bologna, 40126 Bologna, Italy*

Francesco Scarpino − *Dipartimento di Chimica "Giacomo Ciamician", Alma Mater Studiorum Università di Bologna, 40126 Bologna, Italy*

Simona Fermani − *Dipartimento di Chimica "Giacomo Ciamician", Alma Mater Studiorum Università di Bologna, 40126 Bologna, Italy*

Complete contact information is available at: https://pubs.acs.org/10.1021/acssuschemeng.1c01306

Author Contributions

The manuscript was written through contributions of all authors. All authors have given approval to the final version of the manuscript.

Author Contributions

‡These authors contributed equally.

Funding

Italian Minister of University and Research, MIUR ERA-NET Cofund on Blue Bioeconomy (BlueBio) project CASEAWA (Grant Agreement ERA-NET no. 817992).

Notes

The authors declare no competing financial interest.

ACKNOWLEDGMENTS

G.F. and S.F. thank the MIUR ERA-NET for funding and the CIRCMSB for the support.

REFERENCES

(1) Peterson, L. C. Calcium Carbonates. In *Encyclopedia of Ocean Sciences*; Steele, J., Thorpe, S., Turekian, K., Eds.; Academic Press: London, 2019; pp 336−345. DOI: 10.1016/B978-0-12-409548-9.11520-9.

(2) *Calcium Carbonate: From the Cretaceous Period into the 21st Century*; Tegethoff, F. W., Rohleder, J., Kroker, E., Eds.; Birkhauser Velag: Basel, 2001.

(3) Jimoh, O. A.; Ariffin, K. S.; Hussin, H. B.; Temitope, A. E. Synthesis of Precipitated Calcium Carbonate: A Review. *Carbonates Evaporites* **2018**, 33 (2), 331−346.

(4) Teir, S.; Eloneva, S.; Zevenhoven, R. Production of Precipitated Calcium Carbonate from Calcium Silicates and Carbon Dioxide. *Energy Convers. Manage.* **2005**, *46*, 2954−2979.
(5) Meldrum, F. C. Calcium Carbonate in Biomineralisation and Biomimetic Chemistry. *Int. Mater. Rev.* **2003**, *48*, 187−224.
(6) De Reese, J.; Plank, J. Adsorption of Polyelectrolytes on Calcium Carbonate - Which Thermodynamic Parameters Are Driving This Process? *J. Am. Ceram. Soc.* **2011**, *94* (10), 3515−3522.
(7) Shi, X.; Rosa, R.; Lazzeri, A. On the Coating of Precipitated Calcium Carbonate with Stearic Acid in Aqueous Medium. *Langmuir* **2010**, *26* (11), 8474−8482.
(8) Demjén, Z.; Pukánszky, B.; Földes, E.; Nagy, J. Interaction of Silane Coupling Agents with CaCO3. *J. Colloid Interface Sci.* **1997**, *190* (2), 427−436.
(9) Heriyanto; Pahlevani, F.; Sahajwalla, V. Effect of Different Waste Filler and Silane Coupling Agent on the Mechanical Properties of Powder-Resin Composite. *J. Cleaner Prod.* **2019**, *224*, 940−956.
(10) FAO. Yearbook: Fishery and Aquaculture Statistics (Statistics and Information Service of the Fisheries and Aquaculture Department), 2014.
(11) Yan, N.; Chen, X. Don't Waste Seafood Waste: Turning Cast-off Shells into Nitrogen-Rich Chemicals Would Benefit Economies and the Environment. *Nature* **2015**, *524*, 155−157.
(12) Long, X.; Ma, Y.; Qi, L. Biogenic and Synthetic High Magnesium Calcite - A Review. *J. Struct. Biol.* **2014**, *185* (1), 1−14.
(13) Checa, A. G.; Harper, E. M.; González-Segura, A. Structure and Crystallography of Foliated and Chalk Shell Microstructures of the Oyster Magallana: The Same Materials Grown under Different Conditions. *Sci. Rep.* **2018**, *8* (1), 1−12.
(14) Meng, Y.; Fitzer, S. C.; Chung, P.; Li, C.; Thiyagarajan, V.; Cusack, M. Crystallographic Interdigitation in Oyster Shell Folia Enhances Material Strength. *Cryst. Growth Des.* **2018**, *18* (7), 3753−3761.
(15) Hart, A. Mini-Review of Waste Shell-Derived Materials' Applications. *Waste Manage. Res.* **2020**, *38* (5), 514−527.
(16) Morris, J. P.; Backeljau, T.; Chapelle, G. Shells from Aquaculture: A Valuable Biomaterial, Not a Nuisance Waste Product. *Rev. Aquac.* **2019**, *11*, 42−57.
(17) Xiong, X.; Cai, L.; Jiang, Y.; Han, Q. Eco-Efficient, Green, and Scalable Synthesis of 1,2,3-Triazoles Catalyzed by Cu(I) Catalyst on Waste Oyster Shell Powders. *ACS Sustainable Chem. Eng.* **2014**, *2* (4), 765−771.
(18) Zhou, X.; Liu, W.; Tian, C.; Mo, S.; Liu, X.; Deng, H.; Lin, Z. Mussel-Inspired Functionalization of Biological Calcium Carbonate for Improving Eu(III) Adsorption and the Related Mechanisms. *Chem. Eng. J.* **2018**, *351* (April), 816−824.
(19) Kemnitz, K.; Tamai, N.; Yamazaki, I.; Nakashima, N.; Yoshihara, K. Fluorescence Decays and Spectral Properties of Rhodamine B in Submono-, Mono-, and Multilayer Systems. *J. Phys. Chem.* **1986**, *90* (21), 5094−5101.
(20) Weiner, S.; Traub, W.; Miller, A.; Phillips, D. C.; Williams, R. J. P. Macromolecules in Mollusc Shells and Their Functions in Biomineralization. *Philos. Trans. R. Soc. London. B, Biol. Sci.* **1984**, *304* (1121), 425−434.
(21) Marie, B.; Zanella-Cléon, I.; Guichard, N.; Becchi, M.; Marin, F. Novel Proteins from the Calcifying Shell Matrix of the Pacific Oyster Crassostrea Gigas. *Mar. Biotechnol.* **2011**, *13* (6), 1159−1168.
(22) Smith, P. K.; Krohn, R. I.; Hermanson, G. T.; Mallia, A. K.; Gartner, F. H.; Provenzano, M. D.; Fujimoto, E. K.; Goeke, N. M.; Olson, B. J.; Klenk, D. C. Measurement of Protein Using Bicinchoninic Acid. *Anal. Biochem.* **1985**, *150* (1), 76−85.
(23) Bischoff, W. D.; Mackenzie, F. T.; Bishop, F. C. Stabilities of Synthetic Magnesian Calcites in Aqueous Solution: Comparison with Biogenic Materials. *Geochim. Cosmochim. Acta* **1987**, *51* (6), 1413−1423.
(24) Salma-Ancane, K.; Stipniece, L.; Locs, J.; Lakevics, V.; Irbe, Z.; Berzina-Cimdina, L. The Influence of Biogenic and Synthetic Starting Materials on the Properties of Porous Hydroxyapatite Bioceramics. *Key Eng. Mater.* **2014**, *614*, 11−16.
(25) Göppert, A.; Cölfen, H. Infiltration of Biomineral Templates for Nanostructured Polypyrrole. *RSC Adv.* **2018**, *8* (59), 33748−33752.
(26) Beija, M.; Afonso, C. A. M.; Martinho, J. M. G. Synthesis and Applications of Rhodamine Derivatives as Fluorescent Probes. *Chem. Soc. Rev.* **2009**, *38* (8), 2410−2433.
(27) Del Secco, B.; Malachin, G.; Milli, L.; Zanna, N.; Papini, E.; Cornia, A.; Tavano, R.; Tomasini, C. Form Matters: Stable Helical Foldamers Preferentially Target Human Monocytes and Granulocytes. *ChemMedChem* **2017**, *12* (4), 337−345.
(28) Dauphin, Y.; Ball, A. D.; Castillo-Michel, H.; Chevallard, C.; Cuif, J. P.; Farre, B.; Pouvreau, S.; Salomé, M. In Situ Distribution and Characterization of the Organic Content of the Oyster Shell Crassostrea Gigas (Mollusca, Bivalvia). *Micron* **2013**, *44* (1), 373−383.
(29) Dauphin, Y.; Brunelle, A.; Medjoubi, K.; Somogyi, A.; Cuif, J.-P. The Prismatic Layer of Pinna : A Showcase of Methodological Problems and Preconceived Hypotheses. *Minerals* **2018**, *8* (9), 365.
(30) Addadi, L.; Joester, D.; Nudelman, F.; Weiner, S. Mollusk Shell Formation: A Source of New Concepts for Understanding Biomineralization Processes. *Chem. - Eur. J.* **2006**, *12* (4), 980−987.
(31) Herman, A.; Addadi, L.; Weiner, S. Interactions of Sea-Urchin Skeleton Macromolecules with Growing Calcite Crystals- a Study of Intracrystalline Proteins. *Nature* **1988**, *331* (6156), 546−548.
(32) Selvam, P. P.; Preethi, S.; Basakaralingam, P.; Thinakaran, N.; Sivasamy, A.; Sivanesan, S. Removal of Rhodamine B from Aqueous Solution by Adsorption onto Sodium Montmorillonite. *J. Hazard. Mater.* **2008**, *155*, 39−44.
(33) Mohammadi, M.; Hassani, A. J.; Mohamed, A. R.; Najafpour, G. D. Removal of Rhodamine b from Aqueous Solution Using Palm Shell-Based Activated Carbon: Adsorption and Kinetic Studies. *J. Chem. Eng. Data* **2010**, *55*, 5777−5785.
(34) Oyekanmi, A. A.; Ahmad, A.; Hossain, K.; Rafatullah, M. Adsorption of Rhodamine B Dye from Aqueous Solution onto Acid Treated Banana Peel: Response Surface Methodology, Kinetics and Isotherm Studies. *PLoS One* **2019**, *14* (5), 1−20.
(35) Zolotoyabko, E.; Pokroy, B. Biomineralization of Calcium Carbonate: Structural Aspects. *CrystEngComm* **2007**, *9*, 1156−1161.

https://doi.org/10.1021/acssuschemeng.1c01306
ACS Sustainable Chem. Eng. 2021, 9, 6203−6208